



ELSEVIER

Contents lists available at SciVerse ScienceDirect

Comptes Rendus Chimie

www.sciencedirect.com



Full paper/Mémoire

## Synthesis and characterization of $\text{Li}_{1.05}\text{Co}_{1/3}\text{Ni}_{1/3}\text{Mn}_{1/3}\text{O}_{1.95}\text{X}_{0.05}$ (X = Cl, Br) cathode materials for lithium-ion battery

Yuhong Chen<sup>a,\*</sup>, Qishuai Jiao<sup>a</sup>, Liang Wang<sup>b</sup>, Yawei Hu<sup>a</sup>, Na Sun<sup>a</sup>, Yushuang Shen<sup>a</sup>, Yuhua Wang<sup>c</sup>

<sup>a</sup> Department of Chemical and Environmental Engineering, Hebei Chemical and Pharmaceutical Vocational Technology College, Fangxing street, Hebei Shijiazhuang 050026, China

<sup>b</sup> Library of Hebei University of Science and Technology, Hebei Shijiazhuang 050018, China

<sup>c</sup> School of materials science and Engineering, Shijiazhuang Tiedao University, Hebei Shijiazhuang 050043, China

## ARTICLE INFO

## Article history:

Received 4 February 2012

Accepted after revision 7 January 2013

Available online 1 March 2013

## Keywords:

Lithium-ion batteries

Cathode materials

Cl-doped

Br-doped

## ABSTRACT

In order to improve the thermal stability and dynamic performance of  $\text{LiCo}_{1/3}\text{Ni}_{1/3}\text{Mn}_{1/3}\text{O}_2$  materials, Cl-doped and Br-doped materials were synthesized via the co-precipitation method. The morphology, structure, electrochemical performance and thermal stability were characterized by environment scanning electron microscopy (ESEM), X-ray diffraction (XRD), electrochemical impedance spectroscopy (EIS), charge-discharge cycling and differential scanning calorimetry (DSC). Results show that all materials had a stable layered structure with  $\alpha\text{-NaFeO}_2$  and that Cl-doping slightly increased the size of grains. Both Cl-doping and Br-doping improved the high rate of discharge capacity, cycle-life performance and thermal stability, but Cl-doping was better than Br-doping in improving the material structure stability, dynamic performance and thermal stability.

© 2013 Académie des sciences. Published by Elsevier Masson SAS. All rights reserved.

### 1. Introduction

Recently, many researchers have been interested in layered  $\text{LiNi}_{1/3}\text{Mn}_{1/3}\text{Co}_{1/3}\text{O}_2$  for its higher capacity and better safety compared with  $\text{LiCoO}_2$  [1–3]. However, this material has some problems, such as lower discharge performance arising from the lower electronic conductivity and tap density that should be resolved before it can replace  $\text{LiCoO}_2$ . One approach to improve the electrochemical performance is to partially substitute manganese cobalt nickel oxides for transition metals and non-transition metals [4–6]. Another possible approach is to replace oxygen with other elements, such as F [7–9] and S [10,11]. Fluorine substitution for oxygen in lithium nickelate system was pretty effective to obtain reduced impedance, and lattice changes during cycling. Unfortunately, the effect of fluorine on the layered lithium nickelate system was limited

to 4.3 V of charge cut-off limit and the initial discharge capacity was slightly smaller [7–9].

Fluorine, chlorine and bromine are the same group elements and their chemical properties are similar. Compared with fluorine, the chemical property of chlorine is closer to oxygen, so chlorine doping may improve  $\text{LiNi}_{1/3}\text{Mn}_{1/3}\text{Co}_{1/3}\text{O}_2$  material electrochemical performance. According to the literature, the chlorine- and bromine-doped  $\text{LiNi}_{1/3}\text{Mn}_{1/3}\text{Co}_{1/3}\text{O}_2$  materials have not been studied, so in this paper,  $\text{Li}_{1.05}\text{Co}_{1/3}\text{Ni}_{1/3}\text{Mn}_{1/3}\text{O}_{1.95}\text{X}_{0.05}$  (X = Cl, Br) materials were prepared by a co-precipitation method and their structural and electrochemical properties were tested.

### 2. Experimental

#### 2.1. Materials synthesis

The precursor  $\text{Co}_{1/3}\text{Ni}_{1/3}\text{Mn}_{1/3}(\text{OH})_2$  was prepared as extensively detailed in the former references [5,12]. The  $\text{Li}_{1.05}\text{Co}_{1/3}\text{Ni}_{1/3}\text{Mn}_{1/3}\text{O}_{1.95}\text{X}_{0.05}$  (X = Cl, Br) was made by

\* Corresponding author.

E-mail address: chyh76@163.com (Y. Chen).

mixing amounts of LiOH,  $\text{Co}_{1/3}\text{Ni}_{1/3}\text{Mn}_{1/3}(\text{OH})_2$ , and LiCl or LiBr (in the molar ratio of 1:1:0.05), followed by a heat treatment procedure at  $900\text{ }^\circ\text{C}$  for 20 h in a stream of dried air.

## 2.2. Preparation of test cells

A composite electrode was prepared by mixing 85wt%  $\text{Li}_{1.05}\text{Co}_{1/3}\text{Ni}_{1/3}\text{Mn}_{1/3}\text{O}_{1.95}\text{X}_{0.05}$ , 10wt% carbon black as a conductor, and 5wt% PVDF as a binder dissolved in ethanol. The mixed slurry was coated onto Al foil and dried for 12 h. 2032-type simulated cells was employed for electrochemical measurements. The anode was constructed from lithium foil, 1 M  $\text{LiPF}_6$  in EC/EMC/DMC (1:1:1 in weight) was used as electrolyte, and the particular process was shown as in the former literature [5].

## 2.3. Morphology and structure tests

The surface morphology was observed by means of an environment scanning electron microscopy (ESEM, Philips XL-30). Powder X-ray diffraction (XRD) patterns at room temperature were obtained on a Philips X' Pert diffractometer using Co K-alpha radiation.

## 2.4. Electrochemical tests

Electrochemical impedance spectroscopy (EIS) was performed by an electrochemistry working station (Gamry

Instruments). The coin cells were performed galvanostatically at 0.2 C rate or 0.5 C rate, and potentiostatically at 4.3 V until the current dropped to less than 0.01 C, and constant current discharge was enforced at different rates to 2.75 V in the battery tester.

## 2.5. Differential scanning calorimeter tests

In order to obtain the thermal stability of  $\text{Li}_{1.05}\text{Co}_{1/3}\text{Ni}_{1/3}\text{Mn}_{1/3}\text{O}_{1.95}\text{X}_{0.05}$  ( $\text{X} = \text{Cl}, \text{Br}$ ), the cells were charged to 4.3 V. After two days relaxation, the electrode was taken out of the cells in the Ar-filled dry box. It was then washed with DMC, dried thoroughly, and loaded onto an aluminium pan. The aluminium pan was hermetically sealed, placed in an airtight container, and immediately transferred to a DCS instrument (NETZSCH-204). The thermal behavior of the charged compounds was examined up to  $450\text{ }^\circ\text{C}$  at a heating rate of  $10\text{ }^\circ\text{C}/\text{min}$ .

## 3. Results and discussion

### 3.1. Structural properties

The micrographs of the three positive electrode materials were examined using ESEM as shown in Fig. 1. ESEM showed that no morphological change occurred for oxygen substitution with chlorine or bromide and all samples had the particle sizes from 200 to 400 nm. It also can be seen that particle sizes of chlorine-doped materials

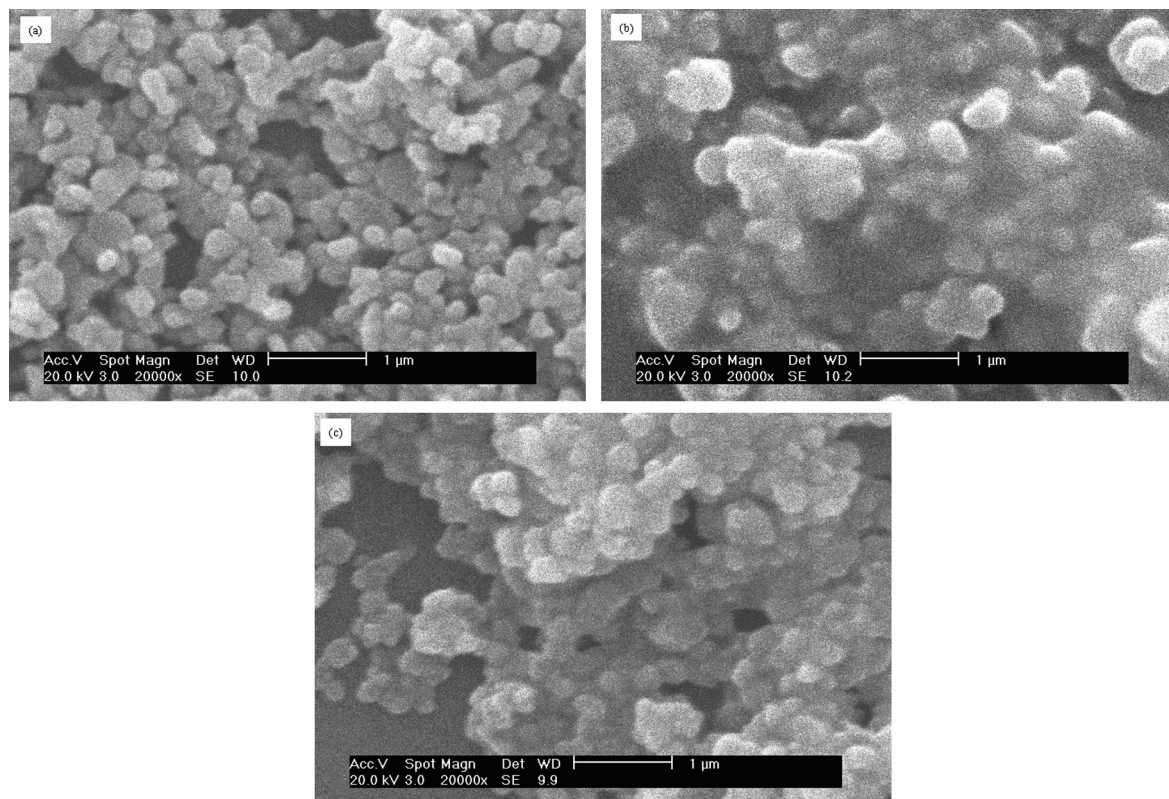


Fig. 1. ESEM images of  $\text{Li}_{1.05}\text{Co}_{1/3}\text{Ni}_{1/3}\text{Mn}_{1/3}\text{O}_{1.95}\text{X}_{0.05}$  ( $\text{X} = \text{Cl}, \text{Br}$ ) powders (a) undoped, (b) chlorine-doped, (c) bromine-doped.

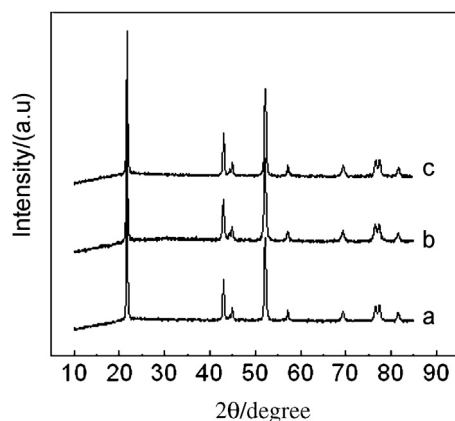


Fig. 2. XRD patterns of  $\text{Li}_{1.05}\text{Co}_{1/3}\text{Ni}_{1/3}\text{Mn}_{1/3}\text{O}_{1.95}\text{X}_{0.05}$  ( $\text{X} = \text{Cl}, \text{Br}$ ) undoped, (b) chlorine-doped (c) bromine-doped.

were slightly larger than that of undoped or bromide-doped materials. For cathode materials of lithium-ion cells, the bigger the particle size was, the more incompact performance and the better fluidity it had, which was propitious to slurry pasting in cathode preparation [9]. The chlorine-doping made the materials form the bigger and denser sinters and was fit for lithium-ion battery preparation.

The XRD patterns of  $\text{Li}_{1.05}\text{Co}_{1/3}\text{Ni}_{1/3}\text{Mn}_{1/3}\text{O}_{1.95}\text{X}_{0.05}$  ( $\text{X} = \text{Cl}, \text{Br}$ ) shown in Fig. 2 can be indexed to a signal phase of  $\alpha\text{-NaFeO}_2$  type with space group  $R\bar{3}m$  [13]. In addition, no other phase's refinement of the XRD profiles, like  $\text{Li}_2\text{O}$  or  $\text{LiX}$ , was present. The hexagonal unit cell parameters calculated for all the products were shown in Table 1. Compared with the undoped sample, the values of  $c$  and  $a$  of chlorine-doped samples decreased and the  $R$  value of chlorine-doped samples increased, which illuminated that chlorine-doping enhanced the layer structure stability and reduced cation mixing [13].

The substitution of chlorine for oxygen should increase lattice parameters, given that the radius of  $\text{Cl}^-$  (1.81 Å) is bigger than that of  $\text{O}^{2-}$  (1.40 Å) [14]. We presume that its appearance should be related to the negative charge decrease during the substitution of chlorine for oxygen in  $\text{LiNi}_{1/3}\text{Mn}_{1/3}\text{Co}_{1/3}\text{O}_2$ . It is well known that the positive charge from transition metal ions should decrease in order to maintain the charge neutrality when  $\text{O}^{2-}$  ions are replaced by  $\text{Cl}^-$ . It may give rise to a reduction in the content of the transition metal ions and results in the reduction of the lattice volume. This results was opposite to those obtained for fluorine-doping [14]. Bromine-doping slightly decreased the lattice parameters and slightly increased the value of  $R$ .

Table 1  
The lattice parameters of the chlorine- and bromine-doped sample.

Sample	$c/\text{nm}$	$a/\text{nm}$	$V$	$I(003)/I(104)$
Undoped	14.371	2.865	102.154	1.39
$\text{Cl}^-$ -doped	14.361	2.862	101.869	1.44
$\text{Br}^-$ -doped	14.372	2.861	102.089	1.41

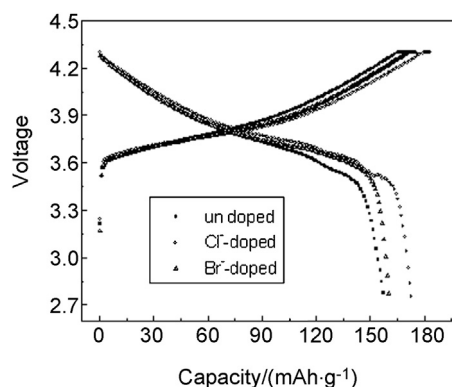


Fig. 3. Third cycles of  $\text{Li}/\text{Li}_{1.05}\text{Co}_{1/3}\text{Ni}_{1/3}\text{Mn}_{1/3}\text{O}_{1.95}\text{X}_{0.05}$  ( $\text{X} = \text{Cl}, \text{Br}$ ) cells at 0.1 C rate between 2.75 V and 4.3 V.

### 3.2. Charge–discharge performance

It can be seen that the charge capacity of undoped, Cl-doped and Br-doped materials was 171.30 mAh/g, 183.41 mAh/g and 175.16 mAh/g, respectively, and the discharge capacity was 157.66 mAh/g, 172.99 mAh/g and 160.39 mAh/g, respectively, which indicated that the discharge capacity was increased by 15.33 mAh/g with Cl-doping and 2.73 mAh/g with Br-doping. The coulombic efficiency of undoped, Cl-doped and Br-doped materials was 92.04%, 94.32% and 91.57%, respectively; this shows that Cl-doping improved the materials reversibility. One reason for better  $\text{Cl}^-$ -doped results may be that chlorine partial replacing oxygen could shrink lattice parameter to enhance structural stability. The other reason may be that Cl-doping could compensate the valence change caused by transition metal ions valence change in cycles (Fig. 3).

Fig. 4 showed the discharge curves of the  $\text{Li}/\text{Li}_{1.05}\text{Co}_{1/3}\text{Ni}_{1/3}\text{Mn}_{1/3}\text{O}_{1.95}\text{X}_{0.05}$  cells at a current density of 0.5 C rate and 1 C rate between 2.75 V and 4.3 V. As shown in Fig. 4a, the discharge capacity of undoped, Cl-doped and Br-doped materials was 136.95 mAh/g, 164.38 mAh/g and 154.75 mAh/g, respectively, and the capacity retention was 86.86%, 95.02% and 96.48%, respectively. As shown in Fig. 4b, the discharge capacity of undoped, Cl-doped and Br-doped materials was 118.48 mAh/g, 158.70 mAh/g and 148.65 mAh/g, respectively, and the capacity retention was 75.14%, 91.74% and 92.68%, respectively. The discharge capacity increased 27.43 mAh/g at a 0.5 C discharge rate and 40.22 mAh/g at a 1 C discharge rate with Cl-doping. It illustrated that Cl-doping improved the materials dynamic performance.

Fig. 5 showed the cycle curves of  $\text{Li}/\text{Li}_{1.05}\text{Co}_{1/3}\text{Ni}_{1/3}\text{Mn}_{1/3}\text{O}_{1.95}\text{X}_{0.05}$  cells at a current density of 1 C charge–discharge rate between 2.75 V and 4.3 V. As shown in Fig. 5, the capacity retentions of the undoped, Cl-doped and Br-doped materials were 74.84%, 91.42% and 81.36%, respectively after 30 cycles. The capacity retention rate increased by 16.56% with Cl-doping and 6.52% with Br-doping at a 1 C charge–discharge rate after 30 cycles. It indicated that Cl-doping and Br-doping could improve the materials' cycle performance at large current charge and discharge rates and Cl-doping was better than Br-doping.

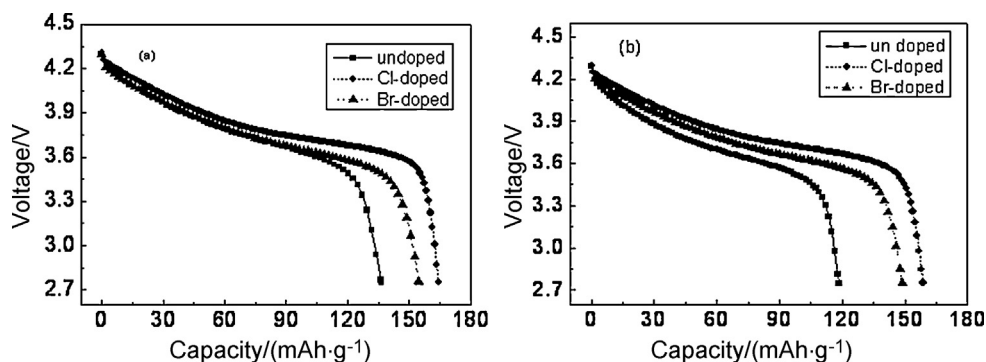


Fig. 4. Effect of chlorine- and bromine-doped on discharge capacity at different current densities (a) 0.5 C, (b) 1 C discharge rates.

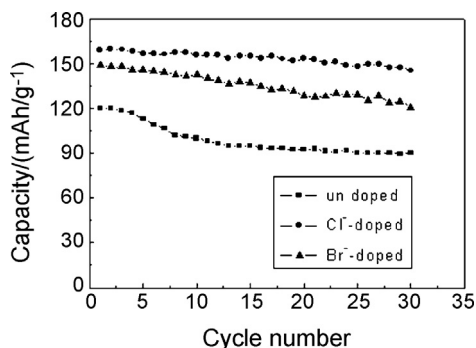


Fig. 5. Cycling performance of Li/Li<sub>1.05</sub>Co<sub>1/3</sub>Ni<sub>1/3</sub>Mn<sub>1/3</sub>O<sub>1.95</sub>X<sub>0.05</sub> (X = Cl, Br) cells.

### 3.3. Electrochemical impedance spectroscopy studies

Fig. 6a compared the impedance spectra of the undoped, Cl-doped and Br-doped samples at a charge potential of 4.3V (vs Li/Li<sup>+</sup>), respectively. There were three parts in the Nyquist curves as shown in Fig. 6a, the high-frequency semicircle was related to the surface film, while the medium-to-intermediate frequency semicircle to the charge transfer process and the interfacial capacitance, and the low-frequency tail to the diffusion of lithium ions in the bulk active mass. Similar impedance patterns were observed for spinel LiMn<sub>2</sub>O<sub>4</sub> as well as for other layered systems [5,12,15,16]. The complex processes occurring

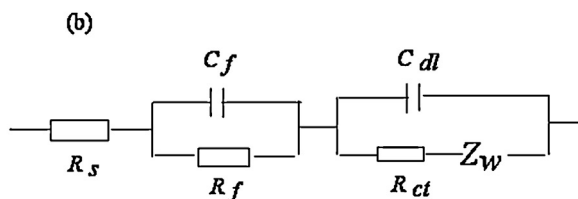
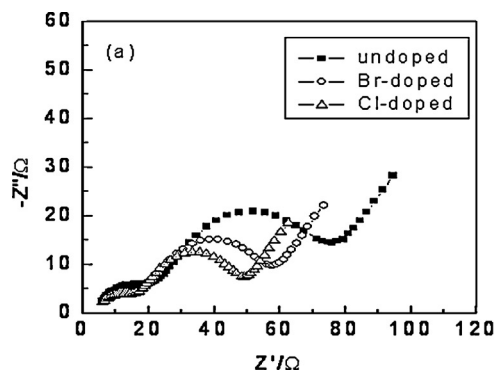


Fig. 6. Nyquist curves of Li<sub>1.05</sub>Co<sub>1/3</sub>Ni<sub>1/3</sub>Mn<sub>1/3</sub>O<sub>1.95</sub>X<sub>0.05</sub> (X = Cl, Br) cathode (a) and equivalent circuit (b).

during intercalation and deintercalation were difficult to understand. It was more convenient to describe them with the equivalent circuit models shown in Fig 6b ( $R_s$ : electrolyte resistance;  $R_f$ : surface film resistance;  $R_{ct}$ : charge transfer resistance;  $C_f$ : surface film capacitance;  $C_{dl}$ : interphase capacitance;  $Z_w$ : Warburg resistance). As shown in Fig. 6a, the medium-to-intermediate frequency semicircle of Cl-doped and Br-doped electrodes was smaller than that of the bare electrode, which indicated that the materials became more conducting with Cl- or Br-doping. It was also seen that line slope of Cl-doped and Br-doped materials was smaller than in the case of undoped samples, which illuminated that the diffusion of lithium ions in Cl-doped or Br-doped materials was quicker [5,15].

### 3.4. Thermal stability studies

To study the thermal stability of Li<sub>1.05</sub>Co<sub>1/3</sub>Ni<sub>1/3</sub>Mn<sub>1/3</sub>O<sub>1.95</sub>X<sub>0.05</sub> (X = Cl, Br), the full charged electrodes were tested by DSC. The exothermic peak represented the reactions between cathode materials and electrolyte; the smaller the exothermic peak area was, the more thermally stable the cathode materials were. As shown in Fig. 7 the Br-doped materials exhibited a small and narrow exothermic peak at 265 °C with an enthalpy of reaction of 753 J/g, the Cl-doped materials exhibited a much smaller and narrower exothermic peak at 295 °C with enthalpy of reaction of 282 J/g. However, the undoped materials exhibited a broad exothermic peak with a much lower

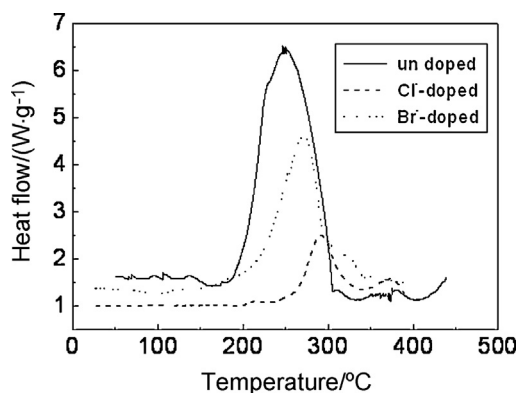


Fig. 7. DSC curves of  $\text{Li}_{1.05}\text{Co}_{1/3}\text{Ni}_{1/3}\text{Mn}_{1/3}\text{O}_{1.95}\text{X}_{0.05}$  ( $\text{X} = \text{Cl}, \text{Br}$ ) electrodes after charged to 4.3 V.

onset temperature at 190 °C and much higher enthalpy of reaction of enthalpy of reaction of 1242 J/g. The enthalpy of reaction decreased 960 J/g and the onset temperature postponed 60 °C approximately with Cl-doping. The enthalpy of reaction decreased 489 J/g approximately with Br-doping. It illuminated that Cl-doping or Br-doping enhanced the material thermal stability and that Cl-doping was better than Br-doping. The reason was that the chemical performance and ionic radii of chlorine were closer to those of oxygen than those of bromine.

#### 4. Conclusion

$\text{Li}_{1.05}\text{Co}_{1/3}\text{Ni}_{1/3}\text{Mn}_{1/3}\text{O}_{1.95}\text{X}_{0.05}$  ( $\text{X} = \text{Cl}, \text{Br}$ ) cathode materials were prepared via the coprecipitation method. We can obtain the following conclusions through XRD, ESEM, DSC and electrochemical tests:

- $\text{Li}_{1.05}\text{Co}_{1/3}\text{Ni}_{1/3}\text{Mn}_{1/3}\text{O}_{1.95}\text{X}_{0.05}$  ( $\text{X} = \text{Cl}, \text{Br}$ ) had a stable layered structure with  $\alpha\text{-NaFeO}_2$  type; Cl-doping improved the structure stability and slightly increased the size of grains;
- the discharge capacity was increased by 15.33 mAh/g with Cl-doping and by 2.73 mAh/g with Br-doping at a 0.1 C discharge rate. The coulombic efficiency improved by 2.18% with Cl-doping;

- Cl-doping was better than Br-doping in improving material dynamic performance. The discharge capacity increased by 27.43 mAh/g at a 0.5 C discharge rate and 40.22 mAh/g at a 1 C discharge rate with Cl-doping. The capacity retention rate increased by 16.56% with Cl-doping at a 1 C charge–discharge rate after 30 cycles;
- Cl-doping or Br-doping enhanced the material thermal stability and the Cl-doping was better than Br-doping. The enthalpy of reaction decreased by 960 J/g and the onset temperature postponed of 60 °C approximately with Cl-doping.

#### Acknowledgment

This project was supported by Natural Science Foundation of youth fund in Hebei Province universities in 2011 (No: 2011211). The authors wish to sincerely acknowledge all assistance from teachers, other students and leaders of McNair New Power Co. Ltd.

#### References

- [1] H. Xia, H.L. Wang, W. Xiao, L. Lu, M.O. Lai, J. Alloys Compd. 480 (2009) 696.
- [2] N. Yabuuchi, T. Ohzuku, J. Power Sources 146 (2005) 636.
- [3] J.T. Su, Y.C. Su, Z.G. Lai, H.H. Yu, Journal of Central South University (Science and Technology) 39 (2009) 19.
- [4] H.J. Li, G. Chen, B. Zhang, J. Xu, Solid State Commun. 146 (2008) 115.
- [5] Y.H. Chen, R.Z. Chen, Z.Y. Tang, L. Wang, J. Alloys Compd. 476 (2009) 539.
- [6] Y.B. Li, B.Z. Chen, H. Xu, X.C. Shi, Y.J. Hu, Y. Chen, Chin. J. of Nonferrous Met. 16 (2006) 1474.
- [7] G.H. Kim, M.H. Kim, S.T. Myung, S.T. Myung, Y.K. Sun, J. Power Sources 146 (2005) 602.
- [8] S.H. Kang, K. Amine, J. Power Sources 146 (2005) 654.
- [9] J.G. Li, C.R. Wan, D.P. Yang, X.P. Yang, Chin. J. Inorg. Mater. 19 (2004) 1298.
- [10] Y.K. Sun, Y.S. Jeon, H.J. Lee, Electrochem. Solid-State Lett. 3 (2000) 7.
- [11] S.H. Park, K.S. Park, Y.K. Sun, K.-S. Nahm, J. Electrochem. Soc. 147 (2000) 2116.
- [12] Y.H. Chen, Z.Y. Tang, G.Q. Zhang, X.M. Zhang, R.Z. Chen, Y.G. Liu, Q. Liu, J. Wuhan University Technology-Mater. Sci. Ed. 23 (2008) 347.
- [13] K.M. Shaju, G.V. Subba Rao, B.V.R. Chowdari, Electrochim. Acta 48 (2002) 145.
- [14] M. Kageyama, D.C. Li, K. Kobayakawa, Y. Sato, Y.S. Lee, J. Power Sources 157 (2006) 494.
- [15] D.S. Lv, W.S. Li, Acta Chim. Sinica 61 (2003) 225.
- [16] G.T.K. Fey, J.G. Chen, V. Subramanian, T. Osaka, J. Power Sources 112 (2002) 384.